ENCLOSURE 2

CNRO-2003-00033

ENGINEERING REPORT M-EP-2003-002, REV. 1

FRACTURE MECHANICS ANALYSIS FOR THE ASSESSMENT OF THE POTENTIAL FOR PRIMARY WATER STRESS CORROSION CRACK (PWSCC) GROWTH IN THE UNINSPECTED REGIONS OF THE CONTROL ELEMENT DRIVE MECHANISM (CEDM) NOZZLES AT ARKANSAS NUCLEAR ONE UNIT 2

Entergy

ENTERGY NUCLEAR SOUTH
Engineering Report Coversheet

Fracture Mechanics Analysis for the Assessment of the Potential for Primary Water Stress Corrosion Crack (PWSCC) Growth in the Un-Inspected Regions of the Control Element Drive Mechanism (CEDM) Nozzles at Arkansas Nuclear One Unit 2

Engineering Report Type:

New ☐ Revision X Deleted ☐ Superceded ☐

Applicable Site(s)

ANO X Echelon X GGNS ☐ RBS ☐ WF3

Report Origin: X ENS ☐ Vendor **Safety-Related:** X Yes ☐ No

Vendor Document No. _____

			Comments:	Attached:
Prepared by:	J. S. Bittner-Lesan Responsible Engineer	Date: 8/26/2003	☐ Yes ☐ No	☐ Yes ☐ No
Verified/ Reviewed by:	Brian C. Gray Design Verifier/Reviewer	Date: 8/26/03	☑ Yes ☐ No	☐ Yes ☑ No
Approved by:	R. L. [illegible] Responsible Supervisor or Responsible Central Engineering Manager (for multiple site reports only)	Date: 8/26/03	☐ Yes ☑ No	☐ Yes ☐ No

Engineering Report No. E-M-EP-2003-002 Rev. 01
Page 2 of 62

RECOMMENDATION FOR APPROVAL FORM

			Comments:	Attached:
Prepared by: J. S. Brahmadesam / William Seino 8/26/03 Responsible Engineer	Date: 8/27/2003		☐ Yes ☐ No	☐ Yes ☐ No
Concurrence: Kirk Tucker Responsible Engineering Manager, ANO	Date: 8/26/03		☐ Yes ☒ No	☐ Yes ☐ No
Concurrence: **Not Applicable** Responsible Engineering Manager, GGNS	Date:		☐ Yes ☐ No	☐ Yes ☐ No
Concurrence: **Not Applicable** Responsible Engineering Manager, RBS	Date:		☐ Yes ☐ No	☐ Yes ☐ No
Concurrence: **Not Applicable** Responsible Engineering Manager, WF3	Date:		☐ Yes ☐ No	☐ Yes ☐ No

Table of Contents

List of Tables

List of Tables (continued)

List of Figures

List of Figures (Continued)

List of Figures (Continued)

List of Appendices

1) Attachment number 32 is intentionally blank, but is included to keep the sequence in order.

Note:- This document {revision 1} was revised to:

1) Make it ANO-2 specific.

2) Revise finite element models and re-analyze residual stresses.

3) Change the surface crack fracture mechanics models.

4) Define augmented inspection regions.

1.0 Introduction

The US Nuclear Regulatory Commission (NRC) issued Order EA-03-009 [1], which modified licenses, requiring inspection of all Control Element Drive Mechanism (CEDM), In-Core Instrumentation (ICI), and vent penetration nozzles in the reactor vessel head. Paragraph IV.C.1.b of the Order requires the inspection to cover a region from the bottom of the nozzle to two (2.0) inches above the J-groove weld. In the Combustion Engineering (CE) design the CEDM nozzles have a guide-cone attached to the bottom of each CEDM. Figure 1 [2] provides a drawing showing the attachment detail and a sketch showing the typical CEDM arrangement in the reactor vessel head. The attachment is a threaded connection with a securing set-screw between the guide-cone and the CEDM nozzle. The CEDM nozzle is internally threaded and the guide-cone has external threads. Thus, the CEDM nozzles in the region of attachment, including the chamfered region, become inaccessible for Ultrasonic Testing (UT) to interrogate the nozzle base material. The design of the UT probes result in a region above the chamfer (0.200 inch [reference 3a &3b]) that cannot be inspected. Therefore, the region of the CEDM base metal that can be inspected begins at about 1.544 inches above the bottom of the CEDM nozzle and extends to two (2.0) inches above the J-groove weld. The unexamined length (here after called the blind zone) constitutes the threaded region, the chamfer region, and the UT dead zone (1.250 + 0.094 + 0.200). The terms used in this report are defined as follows:

- Freespan = (bottom of weld – blind zone); this area below the weld is accessible for volumetric examination.
- Propagation Length = (bottom of weld –top of crack tip); area available for crack growth.

  Note:- for an outside diameter (OD) surface crack, this length is always less than the freespan; for through-wall it is equal to the freespan; and, for an inside diameter (ID) surface crack, the criterion is the propagation length and a through-wall penetration condition.
- Augmented Inspection Area: The axial and circumferential extent of the CEDM below the blind zone subject to an OD surface examination to ensure sufficient region for crack growth in one (1) cycle of operation without compromising the weld. This region may include weld material when the weld extends into the blind zone.

The nozzle as-built dimensions were determined by a detailed review of applicable design drawings and UT data from the previous inspection, which are provided as an attachment in Appendix A. The results of this assessment was used to develop the finite element model which obtains the prevailing stress distribution (Residual+Operating) used in the deterministic fracture mechanics analyses. The deterministic fracture mechanics analyses, in turn, assess the potential for primary water stress corrosion cracking (PWSCC) in the blind zone of the nozzles. This aspect is discussed in more detail in Section 2.

In order to exclude the blind zone from the inspection campaign, a relaxation of the Order is required pursuant to the requirements prescribed in Section IV.F and footnote 2 of the Order [1].

The purpose of this engineering report is to:

1. Determine if sufficient area between the blind zone and the weld exists to facilitate one (1) cycle of axial crack growth without the crack reaching the weld, and
2. For nozzles not meeting 1 above, determine how much of the blind zone combined with the available freespan is required to facilitate 1 cycle of crack growth without the crack reaching the weld. This area is subject to augmented surface examination.

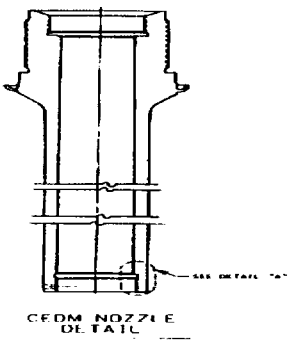

a

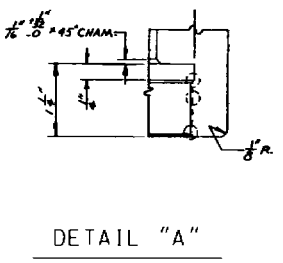

b

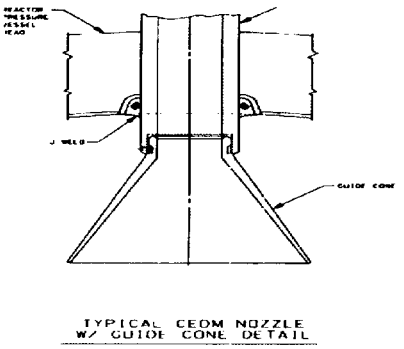

c

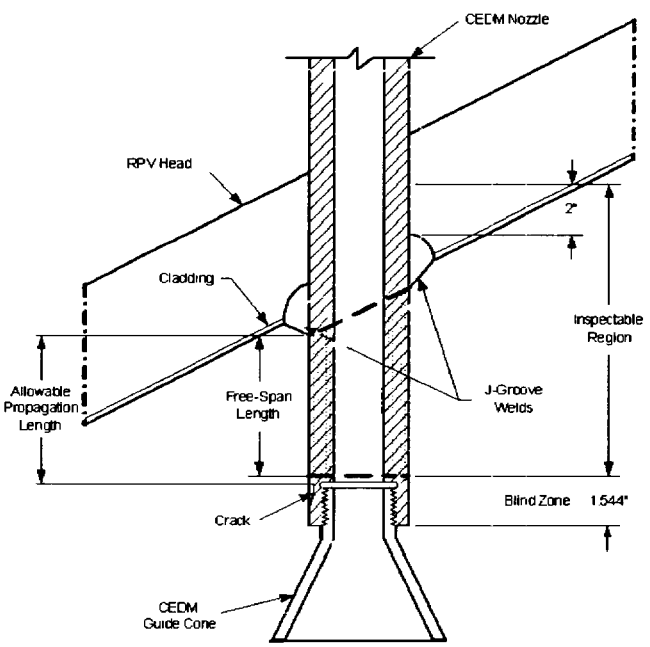

d

Figure 1:

Details of guide cone connection to CEDM[2]. A sketch of a typical CEDM connection showing regions of interest is provided.

a) *CEDM nozzle tube.*

b) Details of the chamfer in the machined recess of the threaded region. Provides dimensions for the threaded and chamfer regions.

c) Details of guide-cone connection to CEDM [2].

d) Sketch of a typical CEDM penetration showing the region of interest.

Detail extracted from Drawing M-2001-C2-23 (ANO-2) [2]. The threaded region in the CEDM is 1.344 inches (Threads plus Recess plus chamfer).

The detail of the guide-cone-to-CEDM connection shows that the threaded + chamfer region is 1.344 inches in height. The UT dead band, determined to be 0.200 inch above the top of the threaded plus chamfer region in the CEDM, is based on a typical inspection probe sled design [3b] (shown in Figure 2).

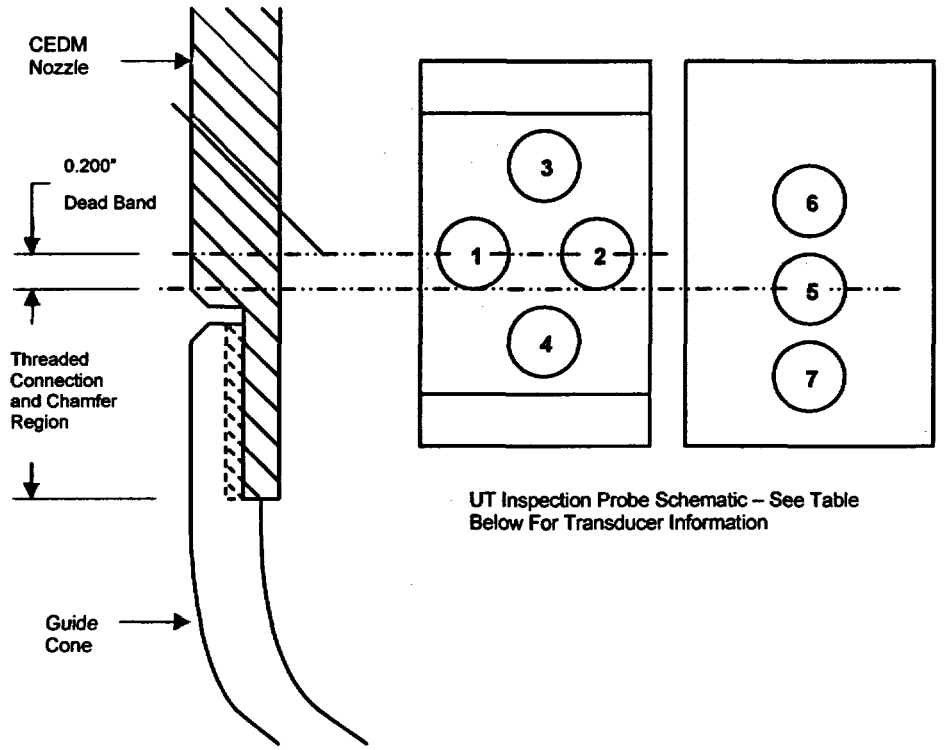

Position	Mode	Diameter	Description
1	Transmit	0.25"	Circumferential Scan Using TOFD
2	Receive	0.25"	Circumferential Scan Using TOFD
3	Transmit	0.25"	Axial Scan Using TOFD
4	Receive	0.25"	Axial Scan Using TOFD
5	Transmit Receive	0.25"	Standard Zero Degree Scan
6	LFEC	NA	Low Frequency Eddy Current Probe
7	EC	NA	Standard Driver/Pickup Eddy Current Probe

Figure 2: *Sketch of a typical inspection probe sled [3a]. The UT dead band is shown with respect to the thread + chamfer region*

Based on the probe design and the geometry of the nozzle at the threaded connection, the explanation provided in Reference 3b shows the UT dead band to

extend 0.200 inch above the chamfer region immediately above the threads. Therefore, to account for the thread region, chamfer and the UT dead band, the blind zone height is determined to be 1.544 inch (1.250" + 0.094" + 0.2") above the bottom of the nozzle.

The analysis used to determine the impact of not examining the blind zone independently evaluates a part through-wall axial crack initiated from the ID, a part through-wall axial crack initiated from the OD, and a through-wall axial crack.

Part Through-Wall Cracks

The initial crack depth obtained from Reference 4 is 0.04627 inch deep for an ID axial crack and 0.07932 inch deep for an OD axial crack. The crack length is based on the detected length of 4 mm (0.157 inch) from Reference 4. In the deterministic fracture mechanics analyses, the part through-wall crack lengths are doubled to 0.32 inch and the crack center is located at the top of the blind zone. Thus, the crack spans both the blind zone and the inspectable region. The postulated crack sizes and depths are two times the detectable limits with one-half (0.16 inch) of the flaw length being located in the examinable area. This provides for a conservative evaluation because:

A) By extending the postulated crack 0.16 inch into the inspectable region, it places the crack tip closer to the weld where the hoop stresses are higher; and

B) it assumes that 0.16 inches of the inspectable region is already cracked, reducing the remaining area for crack propagation.

Through-Wall Crack

In addition to evaluating the part through-wall cracks, this evaluation also conservatively evaluates a through-wall axial crack. The through-wall axial crack is postulated to exist from the top of the blind zone down to a point where the hoop stress is $\leq$ 10 ksi. This is a very conservative assumption, because for a crack to initiate on the surface and propagate through-wall while being totally contained within the blind zone would result in an unrealistic aspect ratio. As can be concluded from the following analysis, the length of a part through-wall crack would propagate into the inspectable region long before its depth reaches a through-wall condition. However, evaluation of the through-wall crack provides completeness to this assessment and ensures all plausible crack propagation modes are considered. Like the part through-wall crack, the hoop stresses at the top of the blind zone were used as the initial stress with adjustments to account for the increased stresses as the crack approaches the weld.

The analyses include a finite element stress analysis of the CEDM nozzles and a fracture mechanics-based crack growth analysis for PWSCC. These analyses are

performed for four nozzles (the nozzles were chosen at four head angles 0°, 8.8°, 28.8°, and 49.6°) in the reactor vessel head to account for the varied geometry of the nozzle penetration. In this manner the analysis provides a bounding evaluation for all nozzles in the reactor vessel head. The sections that follow contain a description of the analyses, the results, and conclusions supported by the analyses.

2.0 Stress Analysis

Finite element-based stress analyses for the ANO-2 CEDM penetrations, using the highest tensile yield strength for each group of nozzles, were performed using the best-estimate geometries based on previous UT and design information. The UT data obtained at the previous refueling outage were reviewed to determine the locations of the top and bottom of the J-weld at two azimuthal locations, downhill (0°) and the uphill (180°). The UT data obtained from this analysis is presented in Appendix A. This UT data were compared to the design information obtained from design drawings using an Excel spreadsheet to estimate the as-built condition. The spreadsheet used in this analysis is presented in Appendix A. This evaluation showed the following:

1) The central CEDM nozzles (0° and 8.8°) have weld sizes that are similar in size to the design drawings. However, this analysis also showed that the nozzle length below the ID clad surface to be 2.08 inches (shorter by 0.4 inch) compared to the design length of 2.48 inches.
2) The downhill side fillet welds on the peripheral CEDM nozzles (28.8° and 49.6°) have a longer leg than estimated from the design information. A fillet weld radius of 3/8 inch instead of the specified 3/16 inch provided the fillet weld leg length that matched the UT data. This evidence was also observed in another CE fabricated reactor vessel head. The fillet weld on the uphill side matched the information on the design drawing. Thus, only the downhill side fillet weld leg was extended for the model. The weld length on the uphill side matched the design information.

The evaluation to estimate the as-built dimensions of the CEDM configuration, taking into consideration the UT data and design information, consisted of the following steps:

1) The blind zone elevation of 1.544 inches from the nozzle bottom was taken to exist for all CEDM nozzles.
2) The design lengths for freespan at both the downhill and uphill locations were established (design length from weld bottom – blind zone).
3) These values were compared to the measurements obtained from the UT data analysis. The differences were recorded.
4) The design length to the top of the J-weld was compared to the measured length from the UT data for both the downhill and uphill locations and the differences recorded.

5) The weld lengths from design drawings were compared to the as measured data from the UT results. This was done for both the downhill and uphill locations. The differences were recorded.

6) The differences were evaluated to assess the variation between the design and as-measured data. This comparison showed that the differences for the central nozzles (8.8°) were consistent but the differences at the uphill location was 0.53 inch and a downhill freespan location was about 0.33 inch. This variation could be reconciled if the nozzle was about 0.4 inch shorter than the design insertion length. Therefore, the design insertion length was reduced by 0.4 inch to minimize the variation between the as-measured and design data. The higher hillside angle nozzles (28.8° and 49.6°) showed the variation to be more on the downhill side indicating a longer fillet weld leg length. This variation was minimized when the fillet weld radius was changed to 3/8 inch instead of the design specified value of 3/16 inch. Similar findings have been observed for another reactor vessel head fabricated by CE. Therefore, the increased fillet weld radius reasonably explains the larger fillet weld leg length observed in the UT data. For these nozzles the fillet weld leg length was increased. Figure 3 presents the sketches for the higher hillside angle nozzles (28.8° and 49.6°). This geometry was used to develop the estimated as-built finite element model. For the central nozzle group (0° and 8.8°), the nozzle insertion length was shortened by 0.4 inch to 2.08 inches. Since the weld lengths measured from the UT data matched the design data, the finite element model was developed using the shorter length but using the as-designed fillet weld dimensions.

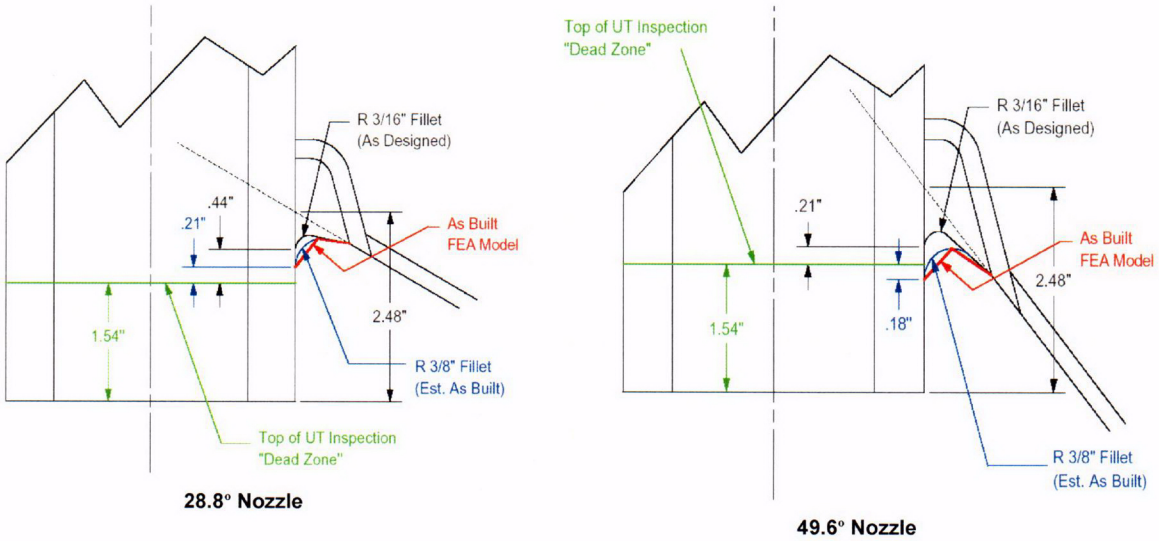

Figure 3: *Estimated as-built nozzle configuration based on evaluation of the UT and design data. For the 49.6° nozzle, the bottom of the fillet weld extends 0.18 inch below the blind zone. For the 28.8° nozzle, the freespan length is reduced to 0.21 inch from the as-designed condition of 0.44 inch.*

C01

The finite element modeling for obtaining the necessary stress (residual+operating) distribution for use in fracture mechanics analysis followed the process and methodology described in Reference 5a. The modeling steps were as follows:

1) The finite element mesh consisted of 3-dimensional solid (brick) elements. Four elements were used to model the tube wall and similar refinement was carried to the attaching J-weld.

2) The CEDM tube material was modeled with a monotonic stress strain curve. The highest yield strength from the nozzle material bounded by the nozzle group was used. This yield strength was referenced to the room temperature yield strength of the stress-strain curve described in Reference 5a. The temperature dependent stress strain curves were obtained by indexing the temperature dependent drop of yield strength.

3) The weld material was modeled as elastic-perfectly plastic for the weld simulation. This approximation is considered reasonable since most of the plastic strain in the weld metal occurs at high temperatures where metals do not work-harden significantly (Reference 5c). The temperature in the weld is always high during the welding process and once the weld begins to cool, the temperatures in the weld at which strain hardening would persist are of limited duration (Reference 5c). This was borne out by the comparison between the analysis based residual stress distribution and that obtained from experiments (Reference 5d).

4) The weld is simulated by two passes based on studies presented in Reference 5a.

5) After completing the weld, a simulated hydro-test load step is applied to the model. The hydro-test step followed the fabrication practice.

6) The model is then subjected to a normal operating schedule of normal heat up to steady state conditions at operating pressure. The residual plus operating stresses, once steady state has been achieved, are obtained for further analysis. The nodal stresses of interest are stored in an output file. These stresses are then transferred to an Excel spreadsheet for use in fracture mechanics analysis.

The stress contours for the four nozzle groups obtained from the finite element analysis are presented in Figures 4 through 7. The stress contour color scheme are as follows:

Dark Navy blue	*from Minimum (Compression) to -10 ksi*
Royal blue	*from -10 to 0 ksi*
Light blue	*from 0 to 10 ksi*
Light green	*from 10 to 20 ksi*
Green	*from 20 to 30 ksi*
Yellow green	*from 30 to 40 ksi*
Yellow	*from 40 to 50 ksi*
Red	*from 50 to 100 ksi*

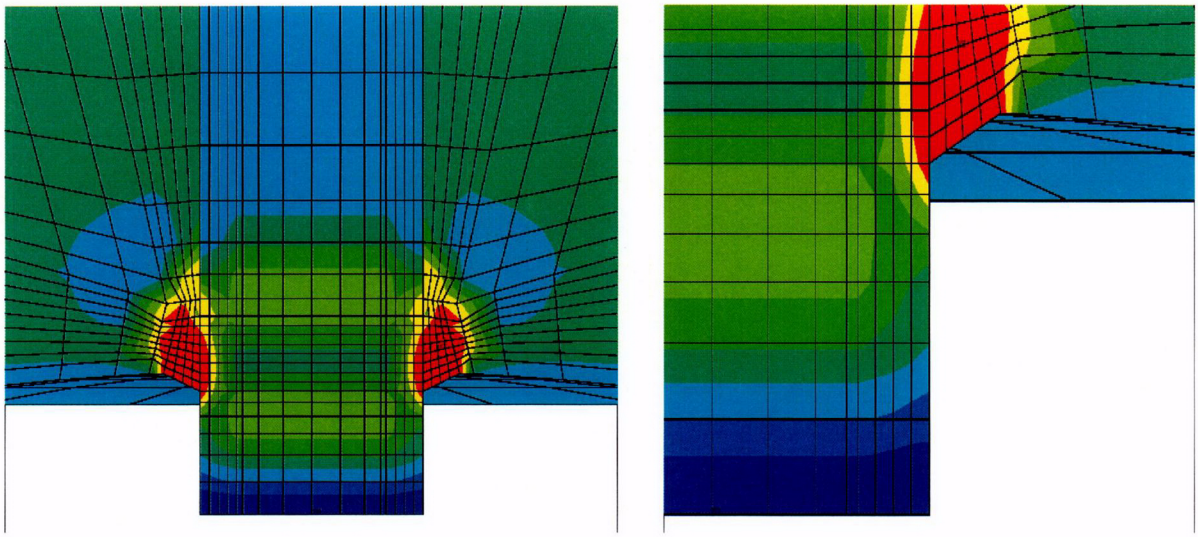

Full Cross-section **Zoomed in right weld**

Figure 4: *Hoop stress contours for the 0° nozzle. High tensile stresses occur in the weld and adjacent tube material. The bottom of the tube is in compression.*

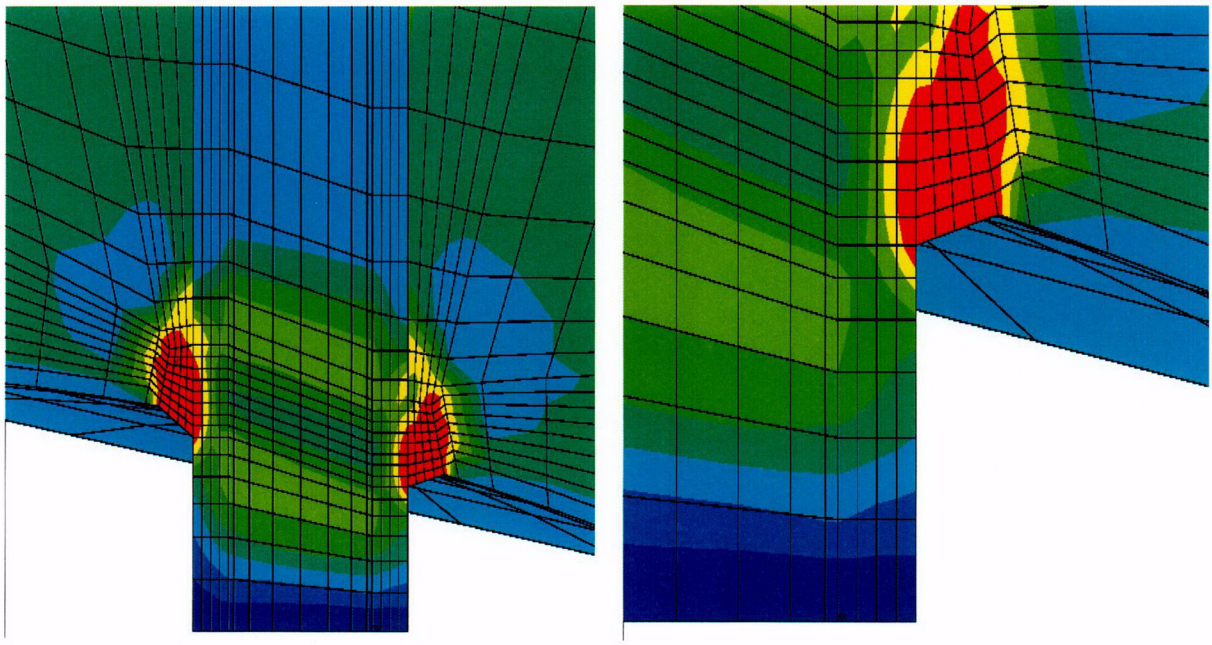

Full cross-section **Zoomed in Downhill side**

Figure 5: *Hoop stress contours for the 8.8° nozzle. High tensile stresses occur in the weld and adjacent tube material. The bottom of the tube is in compression.*

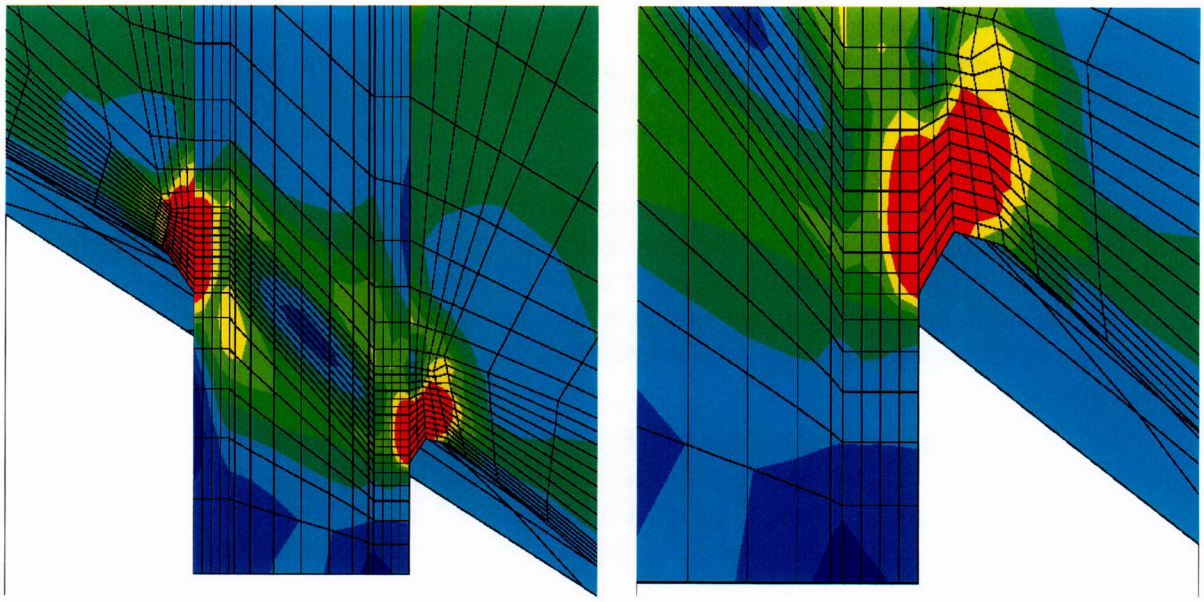

Full cross-section **Zoomed in Downhill side**

Figure 6: *Hoop stress contours for the 28.8° nozzle. High tensile stresses occur in the weld and adjacent tube material. The bottom of the tube is in compression.*

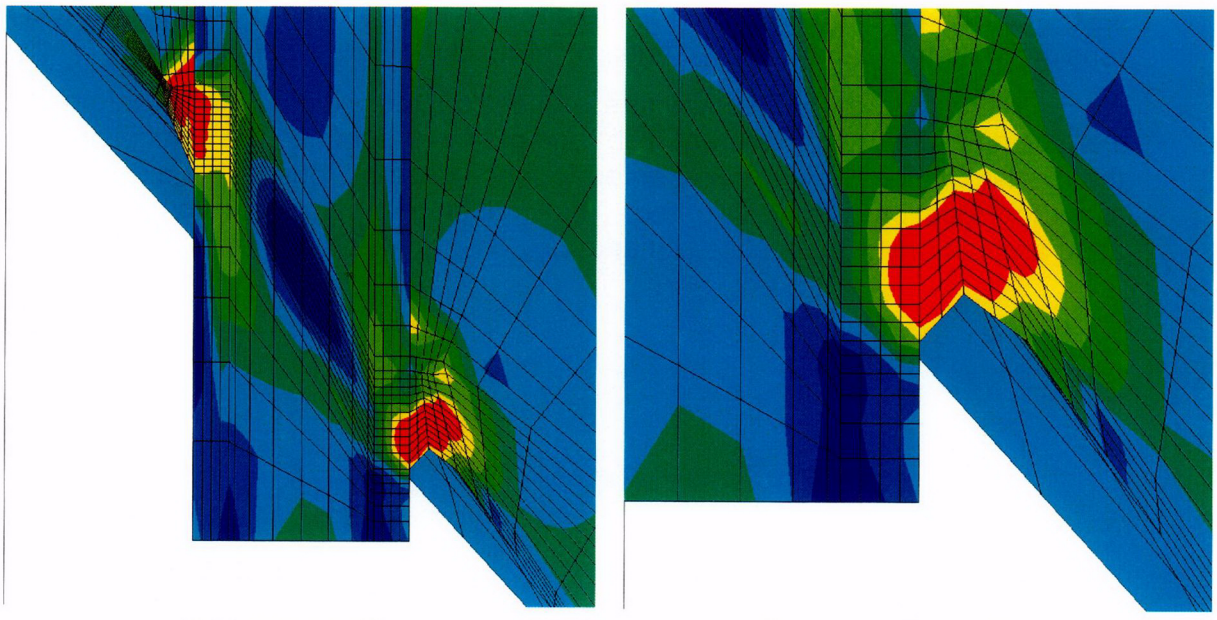

Full cross-section **Zoomed in Downhill side**

Figure 7: *Hoop stress contours for the 49.6° nozzle. High tensile stresses occur in the weld and adjacent tube material. The bottom of the tube is in compression.*

The nodal stresses for the locations of interest in each of the four nozzle groups were provided by Dominion Engineering Inc. and were tabulated in Reference

C03

5b. The nodal stresses and associated figures representing the OD and ID distributions along the tube axis are presented in tables and associated figures in the following pages. The location of the weld bottom was maintained at the node row ending with "601". The blind zone location is shown on the associated figure. For the nozzle group at 8.8°, additional azimuthal locations (22.5°, 45° and 67.5°) around the circumference are shown. For the nozzle group at 28.8°, an additional azimuthal location (22.5°) around the circumference is shown. For the nozzle group at 49.6°, additional azimuthal locations (22.5° and 45°) around the circumference are shown. These additional locations are shown since they were evaluated for establishing the augmented inspection scope. The zone of compressive stress is also marked in the figure.

From the tables and associated figures, a full visualization of the stress distribution in the nozzle, from the nozzle bottom (located at 0.0 inch) to the top of the J-weld is obtained. These figures are also shown in the Mathcad worksheets provided in the Appendix "C" attachments. The nodal stress distribution, provided by Dominion Engineering, is used to establish the region of interest and the associated stress distribution that will be utilized in the subsequent analyses. In all cases evaluated but one, the bottom end of the nozzle (free end) is observed to be in compression. This is expected since the tube in the vicinity of the weld is in tension (high hoop tension), and the normal decay of stresses along the length of the tube results in compressive stress at the bottom. When the weld bottom extends lower, the compressive zone is shortened, but there remains a zone of compressive stress at the free end. For the 49.6° nozzle at the 90° rotated from the downhill location, the ID stress remains in tension while the OD stress becomes compressive (Figure 22)

In the following pages, the stress data from the Excel spreadsheet provided by Dominion Engineering (Reference 5b) and plots representing the axial distribution at the ID and OD locations are presented for each nozzle group with the specific azimuthal location that is evaluated. The location of the compression zone the blind zone and bottom of the weld are marked by colored reference lines.

Row	Height	ID	25%	50%	75%	OD
1	0.000	-25.088	-27.546	-27.787	-25.624	-23.763
101	0.485	-0.56305	-0.53856	-2.1108	-4.851	-6.1565
201	0.874	21.515	18.635	17.122	14.843	10.089
301	1.186	32.751	28.494	24.136	19.645	14.45
401	1.436	35.667	29.598	26.166	25.589	28.417
501	1.635	34.244	29.574	28.286	35.408	45.379
601	1.796	29.45	29.814	31.385	43.337	61.713
701	1.932	23.674	26.502	33.261	47.609	64.65
801	2.068	18.928	24.564	33.968	49.071	65.876
901	2.204	16.541	22.854	34.789	49.525	62.795
1001	2.341	17.561	22.683	33.806	47.49	63.558
1101	2.477	22.026	23.229	32.421	44.118	58.478
1201	2.613	26.382	25.611	31.17	41.606	52.552
1301	2.750	30.043	28.69	33.688	38.959	45.295
1401	2.886	33.132	31.073	37.166	43.676	36.261

Table 1: *Nodal stress for 0° nozzle. This nozzle is symmetric about the nozzle axis hence these stresses prevail over the entire circumference. The weld location is shown by the shaded row.*

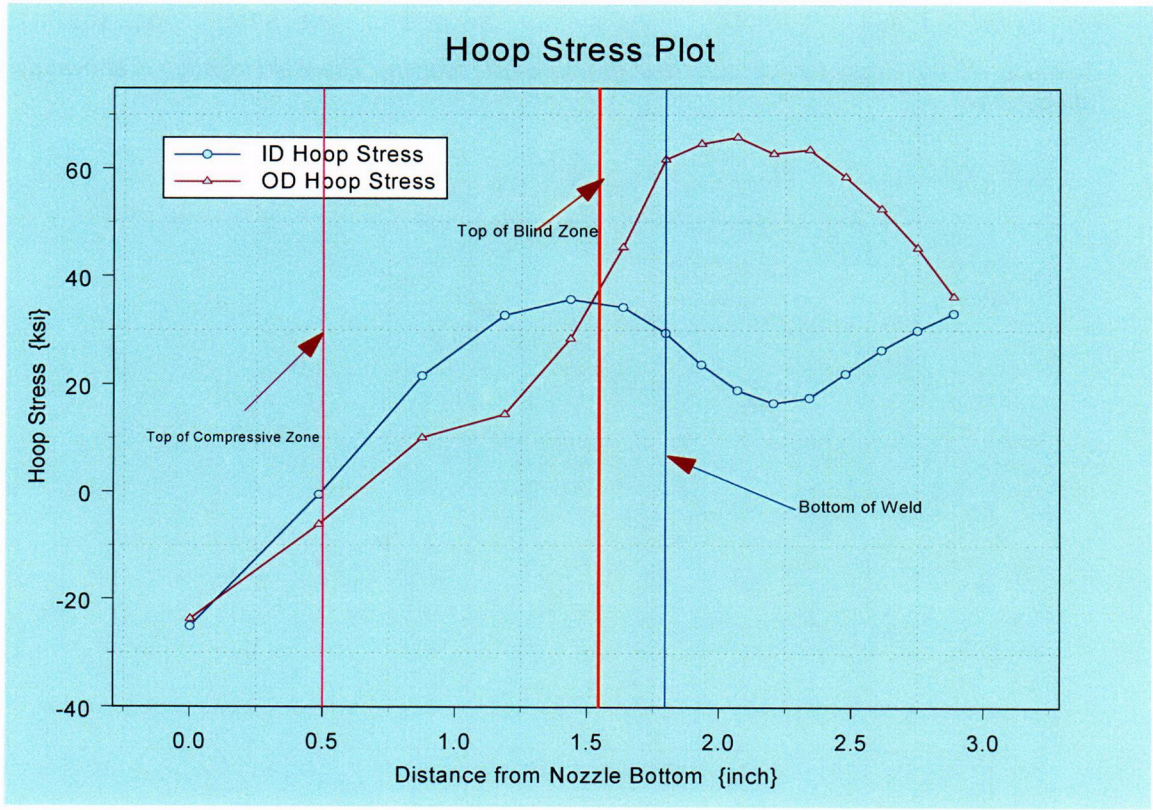

Figure 8: *Plot showing hoop stress distribution along tube axis for the 0° nozzle. The top of compressive zone, the top of blind zone, and the bottom of the weld are shown.*

C04

Row	Height	ID	25%	50%	75%	OD
1	0.000	-27.404	-24.356	-22.209	-20.407	-18.978
101	0.483	0.63328	-1.486	-3.5987	-4.4402	-5.2679
201	0.870	17.665	16.422	14.61	12.415	9.3756
301	1.180	29.798	26.049	22.723	18.95	14.201
401	1.428	33.623	27.792	24.8	24.321	26.989
501	1.627	32.364	28.469	27.591	34.284	45.104
601	1.786	27.394	28.918	31.388	43.882	63.718
701	1.919	21.498	25.556	33.55	48.089	66.365
801	2.051	16.944	23.793	34.064	49.472	67.672
901	2.183	14.834	22.263	34.779	49.055	63.377
1001	2.315	15.852	21.898	33.764	46.61	61.537
1101	2.448	20.835	22.531	32.095	42.501	53.972
1201	2.580	25.973	25.072	30.748	39.365	47.486
1301	2.712	29.955	28.372	32.593	36.879	39.934
1401	2.844	33.46	31.26	36.351	41.573	31.302

Table 2: *Nodal stress for 8.8° nozzle at the downhill location. The weld location is shown by the shaded row.*

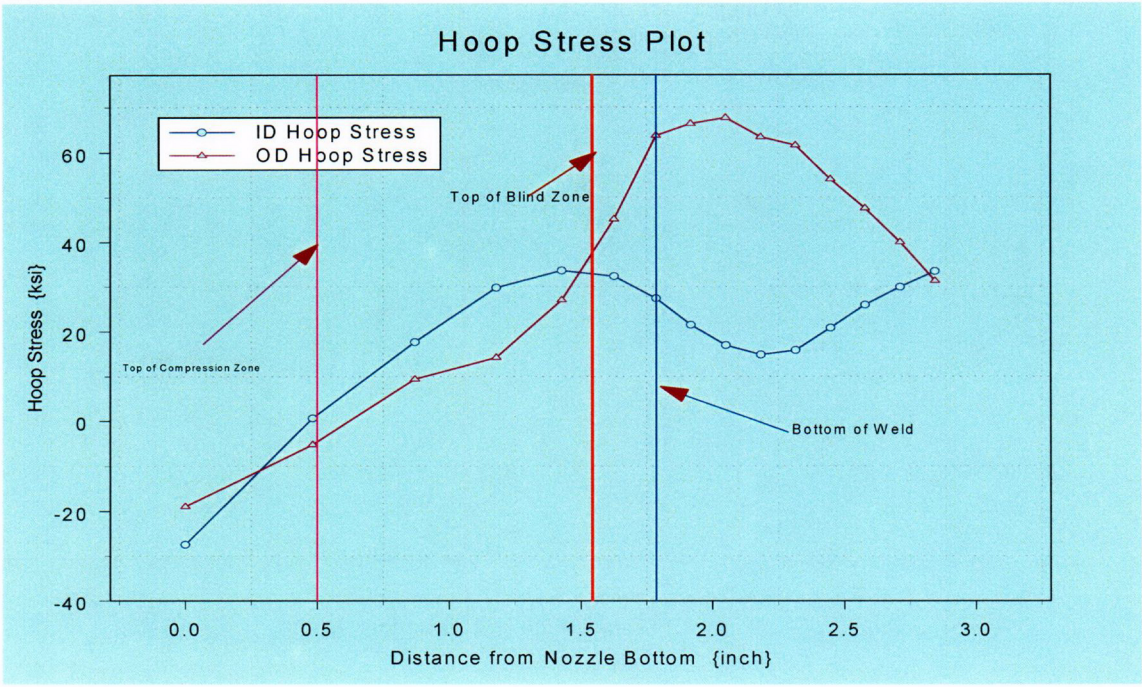

Figure 9: *Plot showing hoop stress distribution along tube axis for the 8.8° nozzle at the downhill location. The top of compressive zone, the top of blind zone, and the bottom of the weld are shown.*

C05

Row	Height	ID	25%	50%	75%	OD
10001	0	-27.118	-24.146	-22.087	-20.358	-18.981
10101	0.48843	0.64978	-1.526	-3.6985	-4.5989	-5.4683
10201	0.87972	17.955	16.435	14.447	12.118	8.9948
10301	1.1932	29.829	26.102	22.672	18.714	13.833
10401	1.4443	33.679	27.823	24.722	24.104	26.541
10501	1.6455	32.389	28.385	27.447	34.121	44.818
10601	1.8067	27.386	28.803	31.156	43.603	61.245
10701	1.9403	21.477	25.458	33.3	47.738	65.934
10801	2.074	16.919	23.701	33.846	49.217	67.244
10901	2.2076	14.769	22.095	34.557	48.869	62.964
11001	2.3413	15.756	21.725	33.561	46.369	61.153
11101	2.4749	20.717	22.317	31.908	42.308	53.889
11201	2.6085	25.789	24.923	30.579	39.284	47.365
11301	2.7422	29.737	28.248	32.847	37.236	40.412
11401	2.8758	33.001	30.843	35.887	41.552	34.5

Table 3: *Nodal stress for 8.8° nozzle at 22.5° rotated from the downhill location. The weld location is shown by the shaded row.*

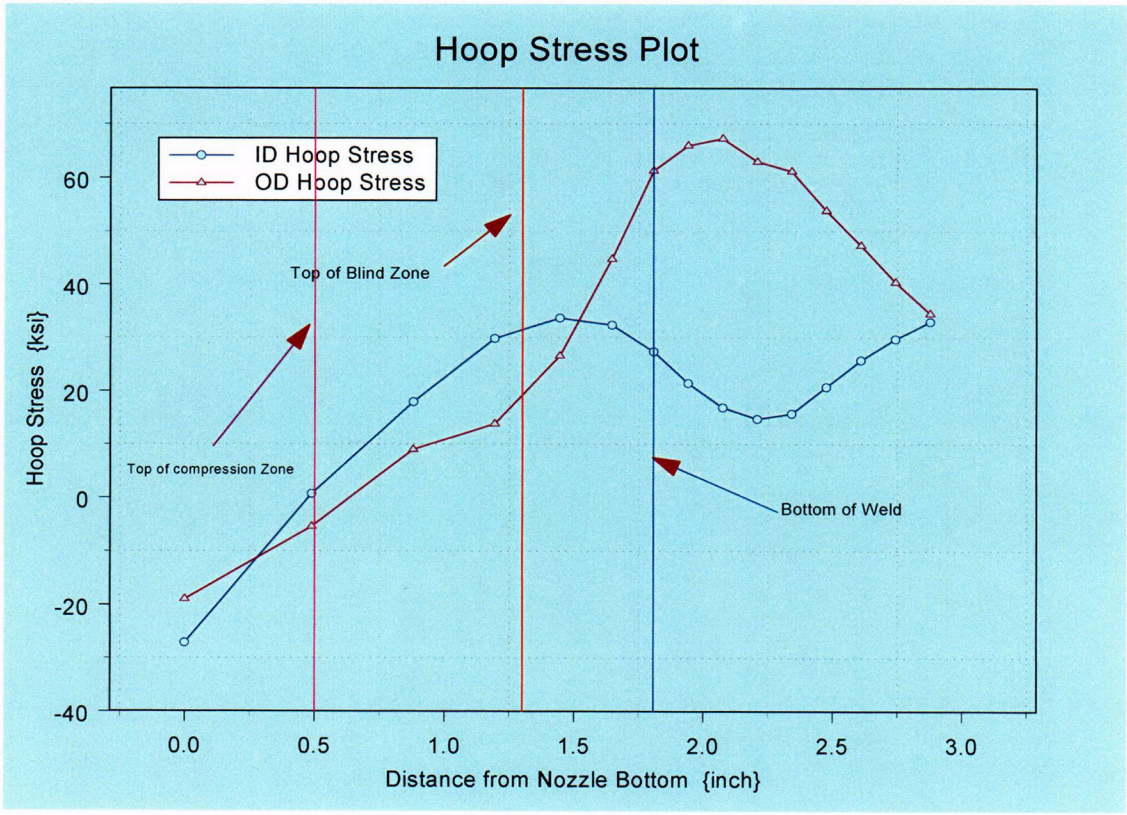

Figure 10: *Plot showing hoop stress distribution along tube axis for the 8.8° nozzle at 22.5° rotated from the downhill location. The top of compressive zone, the top of blind zone, and the bottom of the weld are shown.*

C06

Row	Height	ID	25%	50%	75%	OD
20001	0	-26.311	-23.544	-21.718	-20.18	-18.943
20101	0.50592	-0.3769	-2.2224	-3.9683	-5.0362	-6.0278
20201	0.91123	20.089	16.851	14.017	11.337	7.9165
20301	1.2359	29.934	26.239	22.486	18.067	12.788
20401	1.4961	33.829	27.906	24.526	23.554	25.421
20501	1.7045	32.487	28.206	27.053	33.58	44.169
20601	1.8714	27.432	28.598	30.659	42.946	60.214
20701	2.0063	21.433	25.168	32.645	46.971	64.949
20801	2.1413	16.793	23.322	33.237	48.59	66.19
20901	2.2762	14.561	21.627	33.983	48.342	62.067
21001	2.4111	15.505	21.303	33.027	45.936	60.887
21101	2.5461	20.329	21.914	31.51	42.056	54.174
21201	2.681	25.223	24.532	30.274	39.283	47.704
21301	2.8159	29.209	27.786	32.709	37.408	41.335
21401	2.9509	32.564	30.324	35.521	41.82	35.243

Table 4: *Nodal stress for 8.8° nozzle at 45° rotated from the downhill location. The weld location is shown by the shaded row.*

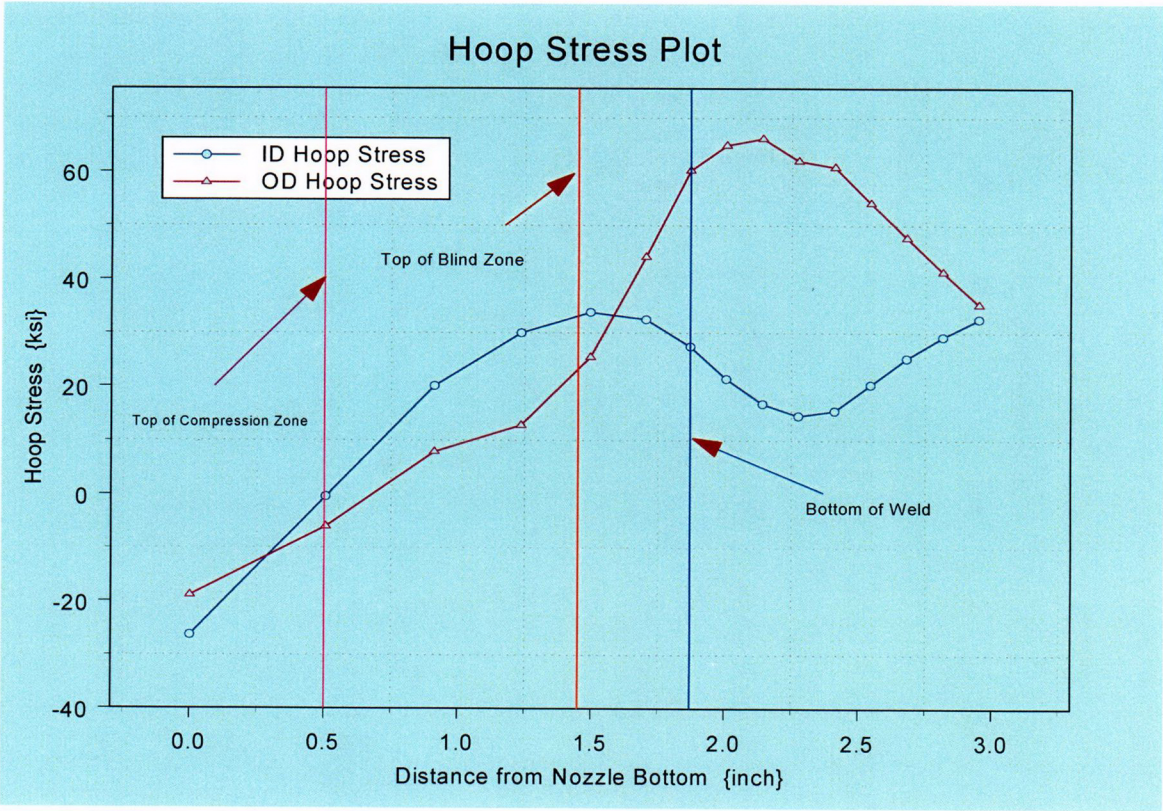

Figure 11: *Plot showing hoop stress distribution along tube axis for the 8.8° nozzle at 45° rotated from the downhill location. The top of compressive zone, the top of blind zone, and the bottom of the weld are shown.*

Row	Height	ID	25%	50%	75%	OD
30001	0	-25.236	-22.713	-21.175	-19.868	-18.802
30101	0.53254	-1.2673	-2.9633	-4.403	-5.6895	-6.8335
30201	0.95918	21.942	17.089	13.361	10.182	6.3275
30301	1.301	30.023	26.373	22.21	17.121	11.241
30401	1.5748	34.094	28.085	24.306	22.834	23.834
30501	1.7941	32.716	28.035	26.605	32.916	43.289
30601	1.9699	27.602	28.447	30.151	42.181	58.888
30701	2.1061	21.457	24.92	31.944	46.103	63.871
30801	2.2422	16.731	22.988	32.591	47.9	65.049
30901	2.3784	14.342	21.261	33.406	47.848	61.204
31001	2.5145	15.204	20.994	32.436	45.675	60.976
31101	2.6507	19.799	21.653	30.997	42.11	55.015
31201	2.7869	24.558	24.206	29.798	39.607	48.995
31301	2.923	28.72	27.503	32.15	37.459	42.682
31401	3.0592	32.844	30.245	35.773	41.844	36.257

Table 5: *Nodal stress for 8.8° nozzle at 67.5° rotated from the downhill location. The weld location is shown by the shaded row.*

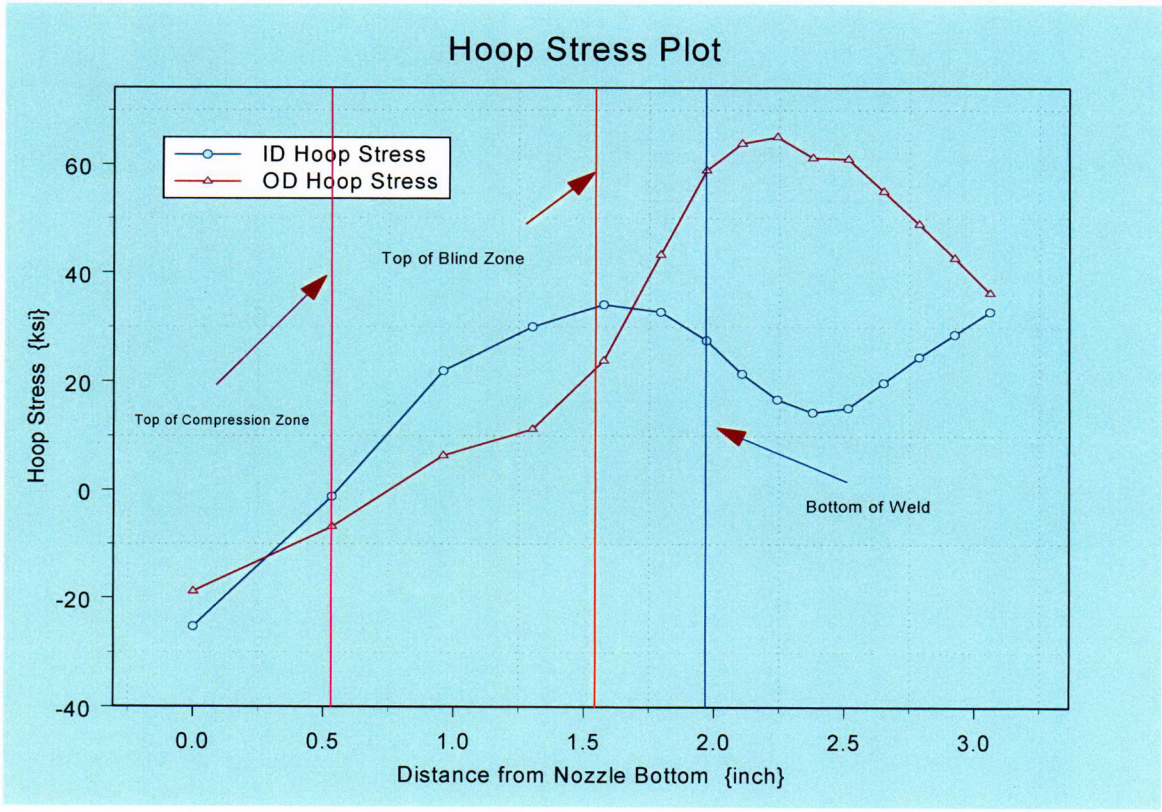

Figure 12: *Plot showing hoop stress distribution along tube axis for the 8.8° nozzle at 67.5° rotated from the downhill location. The top of compressive zone, the top of blind zone, and the bottom of the weld are shown.*

C08

Row	Height	ID	25%	50%	75%	OD
40001	0.000	-24.18	-21.838	-20.55	-19.438	-18.504
40101	0.564	-1.4119	-3.3196	-4.9822	-6.4762	-7.7535
40201	1.016	22.032	16.773	12.529	8.7215	4.4282
40301	1.378	29.956	26.483	21.849	16.053	9.4283
40401	1.668	34.51	28.439	24.198	22.09	22.082
40501	1.900	33.218	28.069	26.319	32.416	42.48
40601	2.087	28.217	28.594	29.911	41.713	57.592
40701	2.224	22.006	25.059	31.606	45.624	63.118
40801	2.361	17.219	23.064	32.349	47.567	64.115
40901	2.499	14.675	21.28	33.218	47.796	60.65
41001	2.636	15.505	21.064	32.273	45.911	61.401
41101	2.773	19.832	21.649	31.008	42.649	56.171
41201	2.911	24.356	24.044	29.89	40.44	50.554
41301	3.048	28.385	27.206	32.287	37.721	43.702
41401	3.185	31.93	29.733	35.809	42.479	38.37

Table 6: *Nodal stress for 8.8° nozzle at (Mid-Plane) 90° rotated from the downhill location. The weld location is shown by the shaded row.*

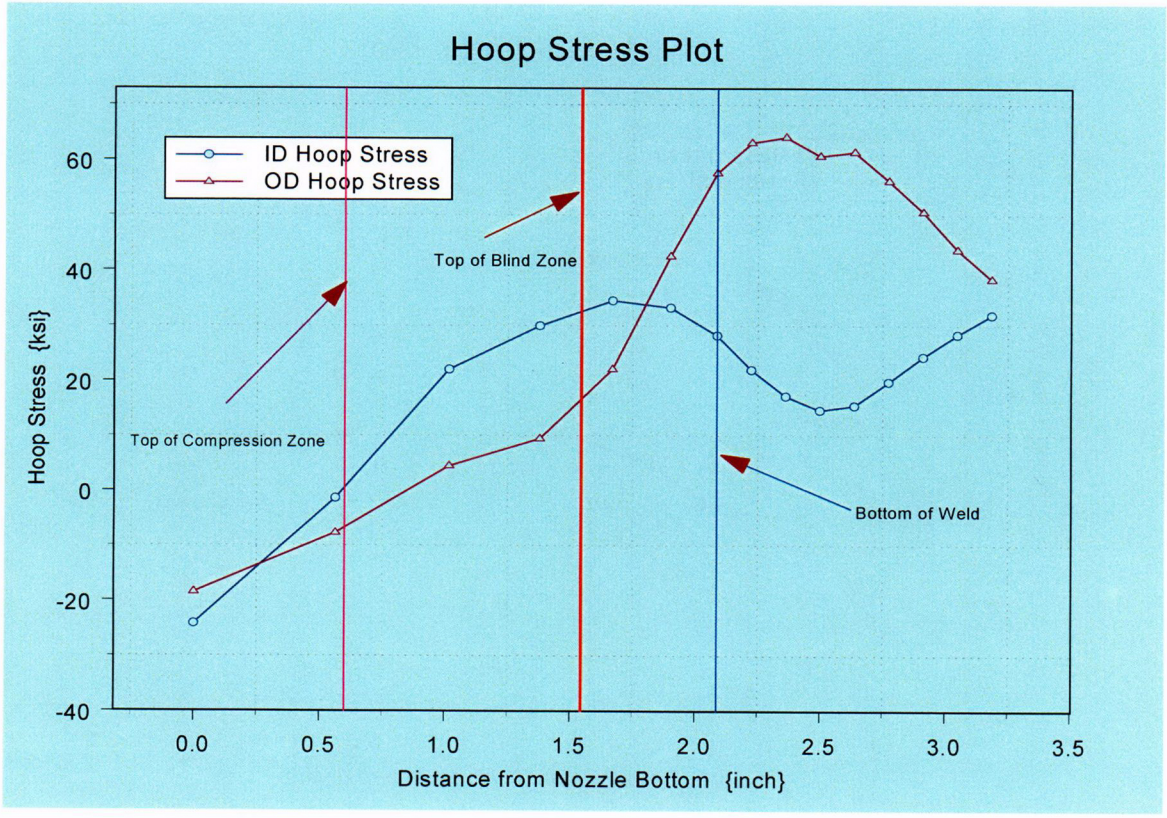

Figure 13: *Plot showing hoop stress distribution along tube axis for the 8.8° nozzle at (Mid-Plane) 90° rotated from the downhill location. The top of compressive zone, the top of blind zone, and the bottom of the weld are shown.*

Row	Height	ID	25%	50%	75%	OD
80001	0.000	-22.34	-20.022	-18.961	-18.087	-17.153
80101	0.645	-0.72174	-3.6673	-6.8206	-8.6957	-10.19
80201	1.162	17.28	14.912	9.6529	3.7661	-1.2205
80301	1.576	29.359	26.501	20.582	13.796	4.7531
80401	1.907	36.503	30.924	25.411	21.15	18.374
80501	2.173	36.536	30.331	27.24	32.606	41.485
80601	2.386	33.132	31.54	31.442	42.452	57.257
80701	2.528	27.116	28.37	33.434	47.233	63.826
80801	2.670	21.957	26.115	34.408	48.851	63.884
80901	2.813	18.993	24.124	35.202	49.904	62.107
81001	2.955	19.578	24.12	34.376	48.405	64.458
81101	3.098	23.12	24.375	33.301	45.647	61.604
81201	3.240	26.499	26.538	32.257	43.763	56.525
81301	3.382	29.872	29.202	35.086	41.634	49.89
81401	3.525	32.509	30.842	37.607	45.45	40.77

Table 7: *Nodal stress for 8.8° nozzle at (Uphill) 180° rotated from the downhill location. The weld location is shown by the shaded row.*

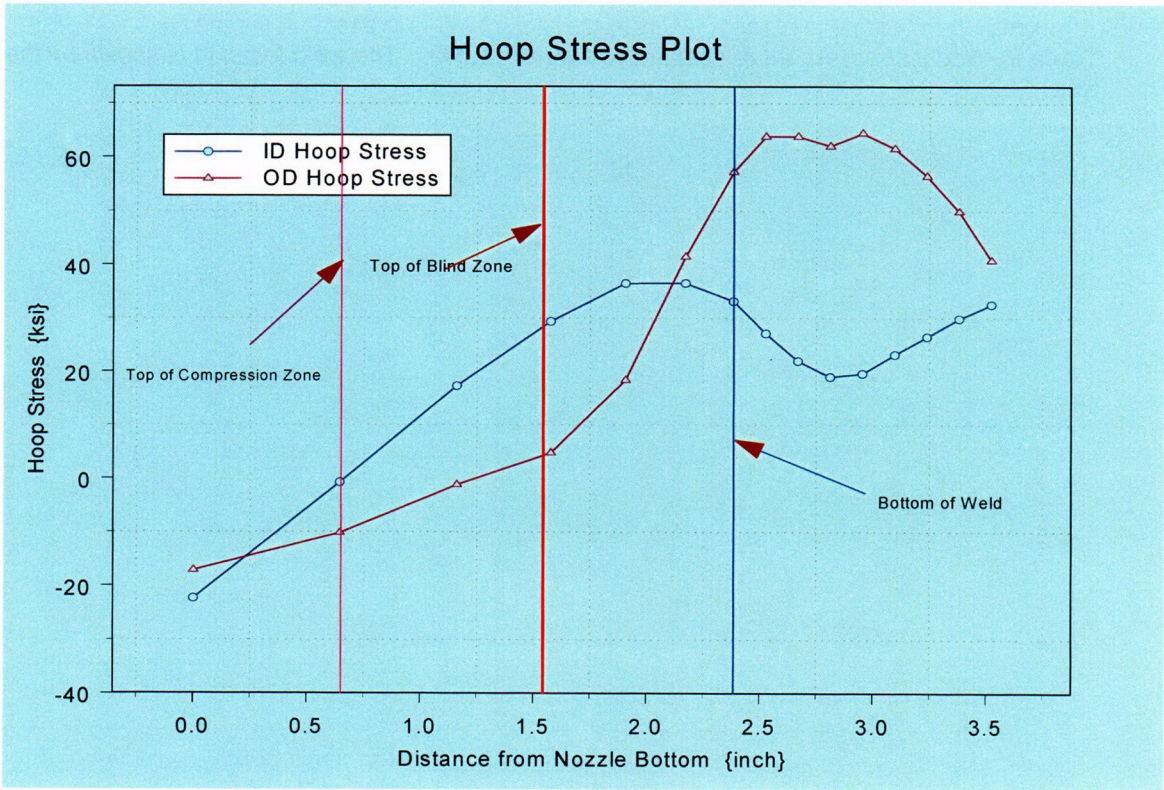

Figure 14: *Plot showing hoop stress distribution along tube axis for the 8.8° nozzle at (Uphill) 180° rotated from the downhill location. The top of compressive zone, the top of blind zone, and the bottom of the weld are shown.*

Row	Height	ID	25%	50%	75%	OD
1	0.000	-17.414	-13.552	-11.113	-8.8843	-6.6283
101	0.461	-8.4943	-6.31	-4.924	-3.7058	-2.5412
201	0.830	0.088906	0.17947	0.11003	0.18625	0.2839
301	1.126	7.0251	6.9534	6.3144	5.2078	4.6462
401	1.363	8.2154	10.954	10.85	9.5121	5.6465
501	1.552	13.266	16.41	16.061	17.131	25.256
601	1.704	20.627	22.237	25.413	43.58	53.784
701	1.825	29.036	28.83	31.285	53.547	64.082
801	1.946	33.945	30.929	36.407	61.6	71.01
901	2.066	29.591	31.788	40.536	64.612	76.418
1001	2.187	23.26	29.738	41.2	64.193	79.626
1101	2.308	18.689	27.734	41.29	61.777	78.117
1201	2.428	15.391	26.097	40.668	58.596	72.784
1301	2.549	14.546	24.118	39.369	54.107	62.074
1401	2.670	16.833	23.402	37.135	47.479	45.328
1501	2.790	22.94	24.557	33.686	39.867	31.733
1601	2.911	30.347	28.824	34.637	35.903	24.215
1701	3.032	36.319	33.178	37.13	37.761	22.663
1801	3.152	40.587	36.14	41.105	36.249	-4.0021

Table 8: *Nodal stress for 28.8° nozzle at downhill location. The weld location is shown by the shaded row.*

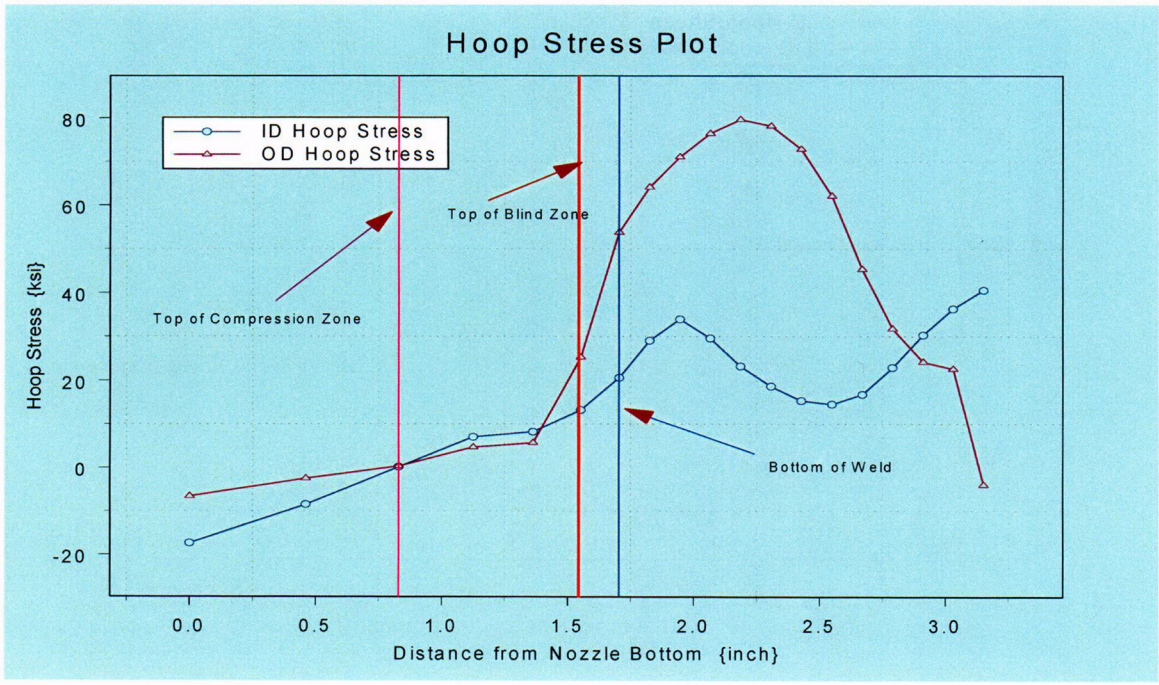

Figure 15: *Plot showing hoop stress distribution along tube axis for the 28.8° nozzle at downhill location. The top of compressive zone, the top of blind zone, and the bottom of the weld are shown.*

Row	Height	ID	25%	50%	75%	OD
10001	0	-14.205	-11.506	-9.7904	-8.2433	-6.7219
10101	0.49517	-6.4931	-5.1879	-4.4249	-3.7959	-3.1762
10201	0.89187	1.5545	1.0213	0.5647	0.25683	-0.0759
10301	1.2097	8.4295	7.9804	7.1986	6.1861	5.292
10401	1.4643	10.247	12.709	12.22	11.35	8.3641
10501	1.6682	15.665	18.335	18.703	20.835	29.697
10601	1.8317	24.321	24.532	26.71	44.525	57.729
10701	1.9511	31.496	28.696	31.228	53.015	63.555
10801	2.0706	31.975	30.109	35.633	59.449	69.026
10901	2.1901	26.833	29.946	38.369	61.124	72.691
11001	2.3096	20.84	27.287	38.5	59.952	75.043
11101	2.4291	15.99	24.671	38.159	58.169	73.854
11201	2.5486	12.461	22.874	37.588	54.954	67.711
11301	2.6681	11.21	20.931	36.521	51.142	59.155
11401	2.7876	13.526	20.476	34.299	45.784	43.711
11501	2.9071	19.78	22.135	31.566	38.968	31.028
11601	3.0266	26.712	26.192	32.945	36.476	24.484
11701	3.1461	32.478	30.015	35.497	38.328	23.185
11801	3.2656	36.911	32.504	38.269	35.608	2.1982

Table 9: *Nodal stress for 28.8° nozzle at 22.5° rotated from the downhill location. The weld location is shown by the shaded row.*

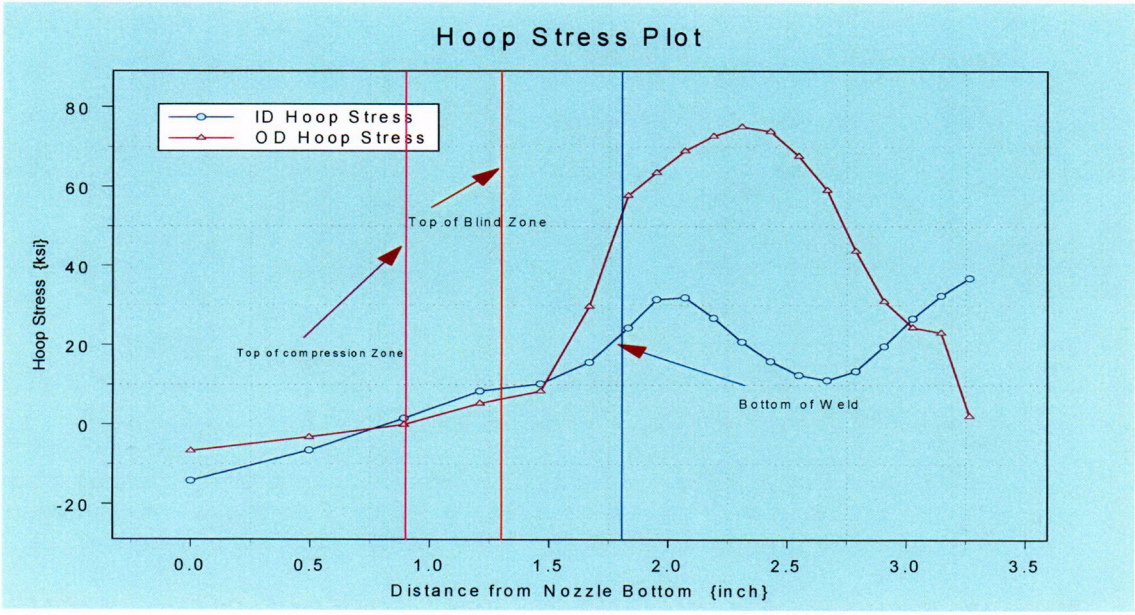

Figure 16: *Plot showing hoop stress distribution along tube axis for the 28.8° nozzle at 22.5° rotated from the downhill location. The top of compressive zone, the top of blind zone, and the bottom of the weld are shown.*

C12

Row	Height	ID	25%	50%	75%	OD
40001	0.000	2.0791	-0.87476	-2.9601	-4.82	-6.7498
40101	0.811	0.091	-2.3704	-4.267	-6.0042	-7.5523
40201	1.460	5.2826	1.6859	-0.78573	-2.4896	-3.4686
40301	1.980	16.881	12.419	9.564	6.9075	4.3191
40401	2.397	24.144	20.894	18.115	16.59	14.513
40501	2.731	26.962	22.672	20.686	24.842	33.523
40601	2.999	23.279	20.902	21.706	37.111	47.395
40701	3.113	17.161	17.101	20.743	41.091	51.762
40801	3.228	11.722	14.424	21.34	43.543	53.688
40901	3.343	6.0041	11.108	20.912	43.833	54.154
41001	3.457	1.439	8.0852	20.38	43.021	57.025
41101	3.572	-2.1749	5.8905	19.929	42.405	56.415
41201	3.687	-4.7249	4.8584	19.994	40.425	58.85
41301	3.801	-4.9201	4.8793	20.34	38.451	57.617
41401	3.916	-2.8845	6.4727	20.545	37.523	49.152
41501	4.031	0.86049	8.0075	21.386	36.18	40.228
41601	4.145	5.584	11.001	22.915	36.59	35.152
41701	4.260	9.8086	14.62	25.477	36.977	32.699
41801	4.375	17.392	18.195	28.176	40.112	19.759

Table 10: *Nodal stress for 28.8° nozzle at (Mid-Plane) 90° rotated from the downhill location. The weld location is shown by the shaded row.*

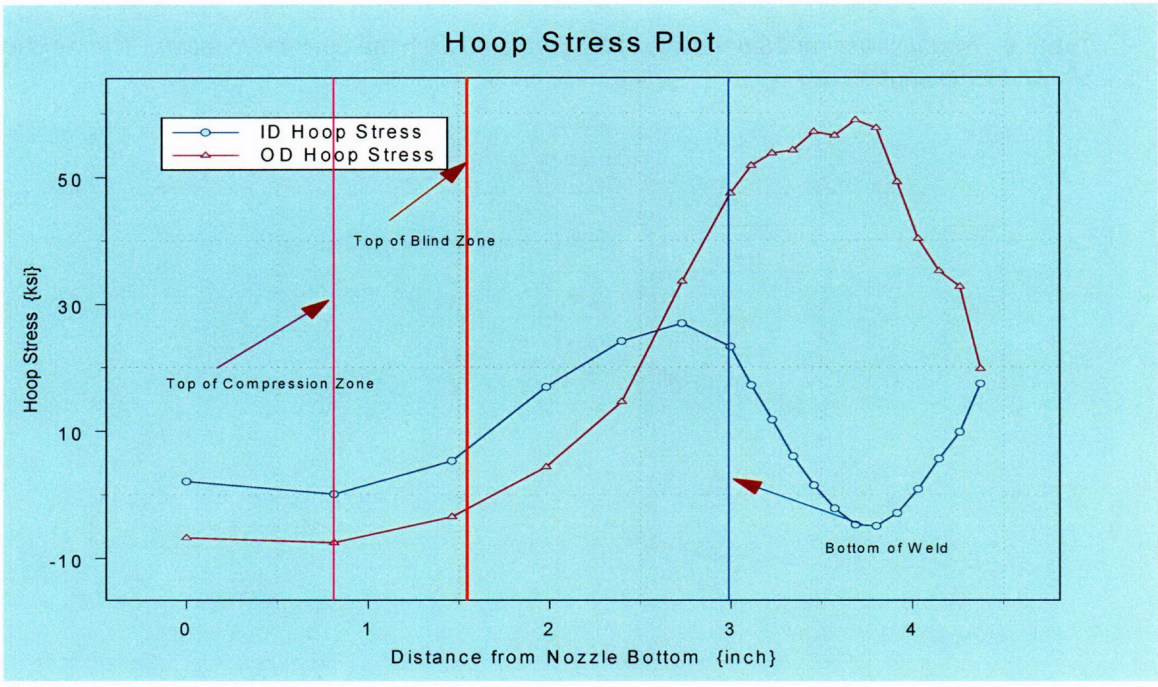

Figure 17: *Plot showing hoop stress distribution along tube axis for the 28.8° nozzle at (Mid-Plane) 90° rotated from the downhill location. The top of compressive zone, the top of blind zone, and the bottom of the weld are shown.*

Row	Height	ID	25%	50%	75%	OD
80001	0.000	-9.0335	-5.8552	-4.2456	-2.6894	-1.0312
80101	1.154	-6.761	-6.7389	-7.2366	-7.6623	-7.8035
80201	2.078	7.9654	1.7419	-6.2304	-11.848	-16.387
80301	2.819	23.851	21.763	8.5552	-6.3899	-17.647
80401	3.412	43.99	38.072	29.826	13.47	-1.6316
80501	3.888	47.954	41.753	35.453	33.324	35.846
80601	4.268	43.756	39.214	38.4	53.023	57.543
80701	4.377	40.773	36.237	41.27	61.453	62.189
80801	4.486	39.277	35.327	44.863	64.204	63.895
80901	4.595	36.022	35.389	46.842	64.323	62.934
81001	4.704	33.54	36.173	48.06	64.483	66.03
81101	4.813	32.631	36.616	47.779	67.612	70.356
81201	4.922	32.794	36.656	47.356	66.386	72.973
81301	5.031	33.889	36.612	47.548	65.375	77.806
81401	5.140	35.222	36.179	47.538	65.411	75.322
81501	5.249	36.353	35.865	47.964	64.448	70.447
81601	5.358	36.426	36.986	48.341	62.979	62.511
81701	5.467	37.233	38.52	49.064	63.153	61.112
81801	5.575	40.874	39.218	48.17	62.039	57.291

Table 11: *Nodal stress for 28.8° nozzle at (Uphill) 180° rotated from the downhill location. The weld location is shown by the shaded row.*

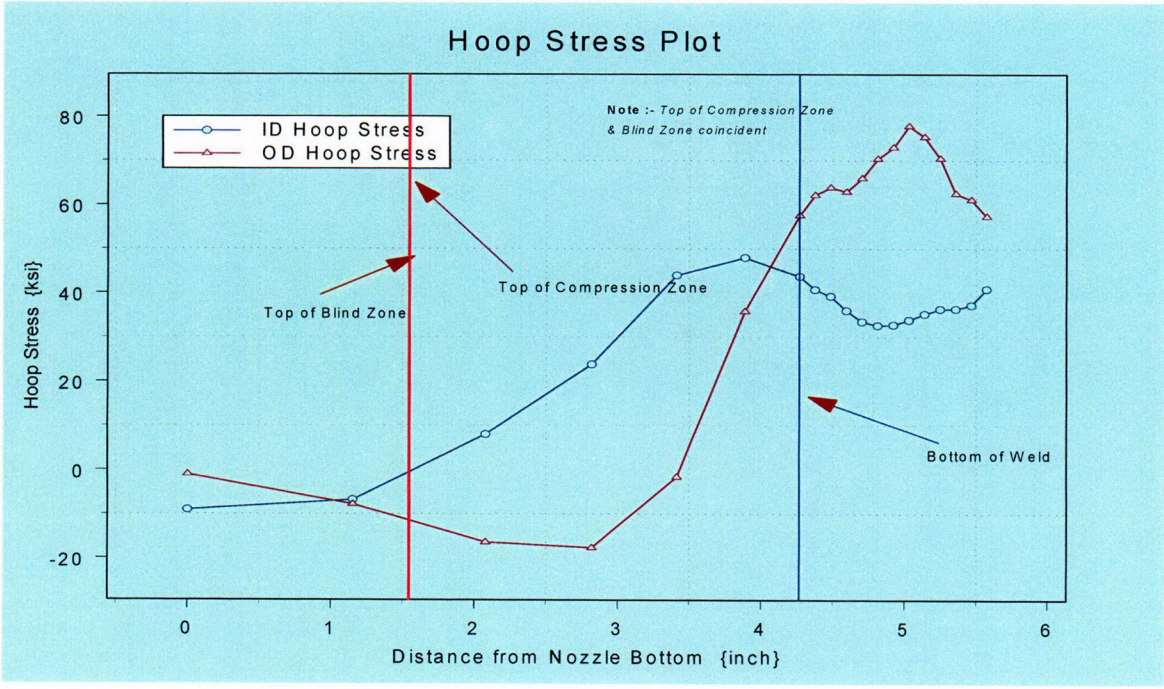

Figure 18: *Plot showing hoop stress distribution along tube axis for the 28.8° nozzle at (Uphill) 180° rotated from the downhill location. The top of compressive zone, the top of blind zone, and the bottom of the weld are shown.*